Field Solver Test

Sandroos, Arto

20.5. 2011

1 Introduction

The purpose of the test was to demonstrate that the field solver works, and to test the effects of grid refinement and increase of the order of accuracy of the solver on the results. The field solver is developed by Londrillo and del Zanna [1].

Part I
Solver Accuracy and Correctness

2 Test Case

Field solver test was made by using a simple advection setup in a $(x, y, z) \in [-1, 1] \times [-1, 1] \times [-1, 1]$ grid and by using periodic boundary conditions. The initial condition was $B_x = 1$ in $(y, z) \in [-0.25, 0.25] \times [-0.25, 0.25]$ and zero elsewhere. The field was then propagated with a constant velocity $\mathbf{V} = (0, -1, -1)$.

Test case was run with two different cell sizes, 10×10 (sparse) and 20×20 (dense). Time step in sparse grid was $\Delta t = 0.05$ and in total 40 time steps were calculated. In dense grid the time step was halved, $\Delta t = 0.025$ and in total 80 time steps were calculated. The time step was chosen in such a way that at the end of simulation the advected field was back at its initial position.

3 Results

Figures 1-6 show selected results from field solver test in sparse and dense grid, and with 1^{st}- and 2^{nd}-order accurate solvers. In 2^{nd}-order accurate cases three different slope limiters were used (minmod, MC limiter, Van Leer).

Formal demonstration of solver accuracy would be made by comparing the solutions against the initial state after a full period and by calculating the L^1 error norms. Here the peak value of B_x at the end of simulation is used as a proxy for solver accuracy instead. The L^1 error norms are not diffucult to calculate in this case, however.

Solver	sparse grid	dense grid
1^{st}	8.33%	16.1%
2^{nd} (minmod)	21.2%	50.6%
2^{nd} (MC limiter)	38.7%	93.1%
2^{nd} (Van Leer)	15.7%	34.4%

Table 1: Peak value of B_x, as percentage of initial value, with different solver versions in sparse and dense grid.

The results indicate that moving into 2^{nd}-order accuracy has a larger impact on the quality of the solution than doubling of the grid size (which is what adaptive mesh refinement effectively does). Obviously the best results were obtained with a 2^{nd}-order accurate solver in denser grid. The results are summarized in Table 1.

Part II
Boundary Conditions

4 Test Case

The test case used to verify that boundary conditions work is the same as used for solver correctness (Sect. 2). Here we are propagating B_x to $(-y, +z)$ direction with a constant velocity. When the field is hits the boundary, it should flow through. Also the values of face-averaged B on "dummy faces" must not effect the solution inside the simulation domain - here B on dummy faces was set to value 666.

Figure 7 shows the numerical solution after 10, 20, and 80 time steps. Evidently the dummy faces do not affect the solution as there are no visible artifacts. The initial (physical) magnetic field also propagates neatly through the corner of the simulation domain. Figure 8 shows the numerical solutions at the same time steps for a 2^{nd}-order accurate solver version. Again, no visible artifacts are present indicating that the boundaries are working as expected. The solution is also less diffusive than the one calculated with 1^{st}-order accurate solver (compate the rightmost panels on Figs. 7 and 8).

References

[1] Londrillo and del Zanna, J. Comp. Phys., 195, 2004.

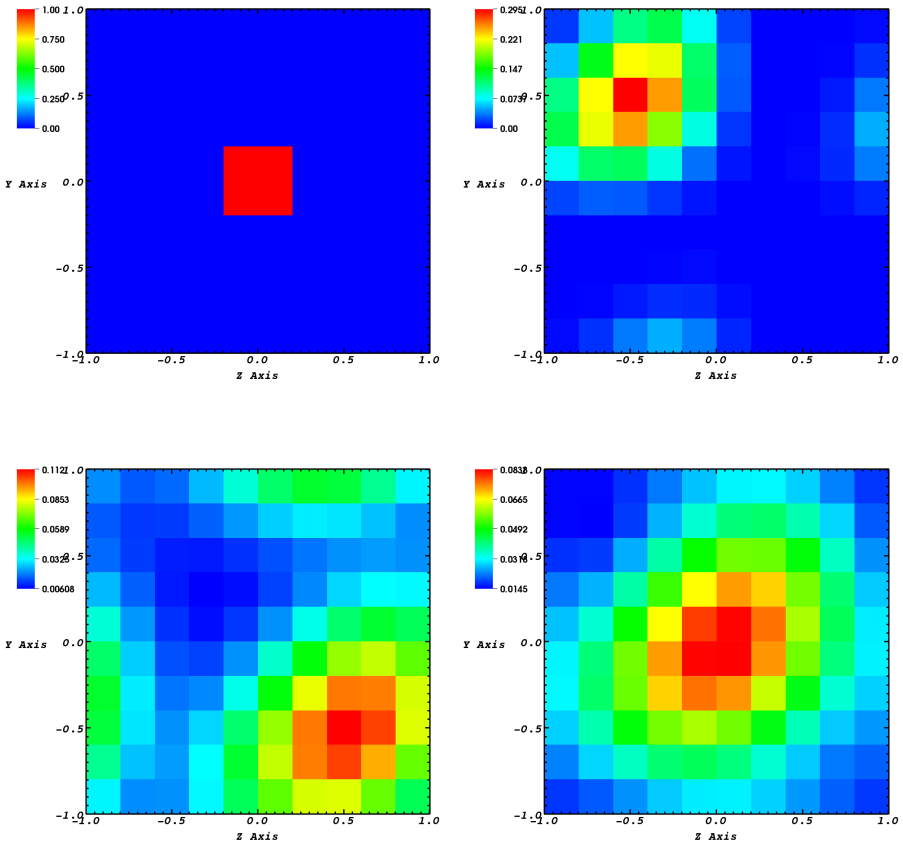

Figure 1: Propagation of B_x with a 1$^{\text{st}}$-order accurate field solver in a sparse grid. The pictures show the initial state, and solutions after 10, 30, and 40 time steps with periodic boundary conditions. Maximum value at 40 time steps is 8.33% of initial value.

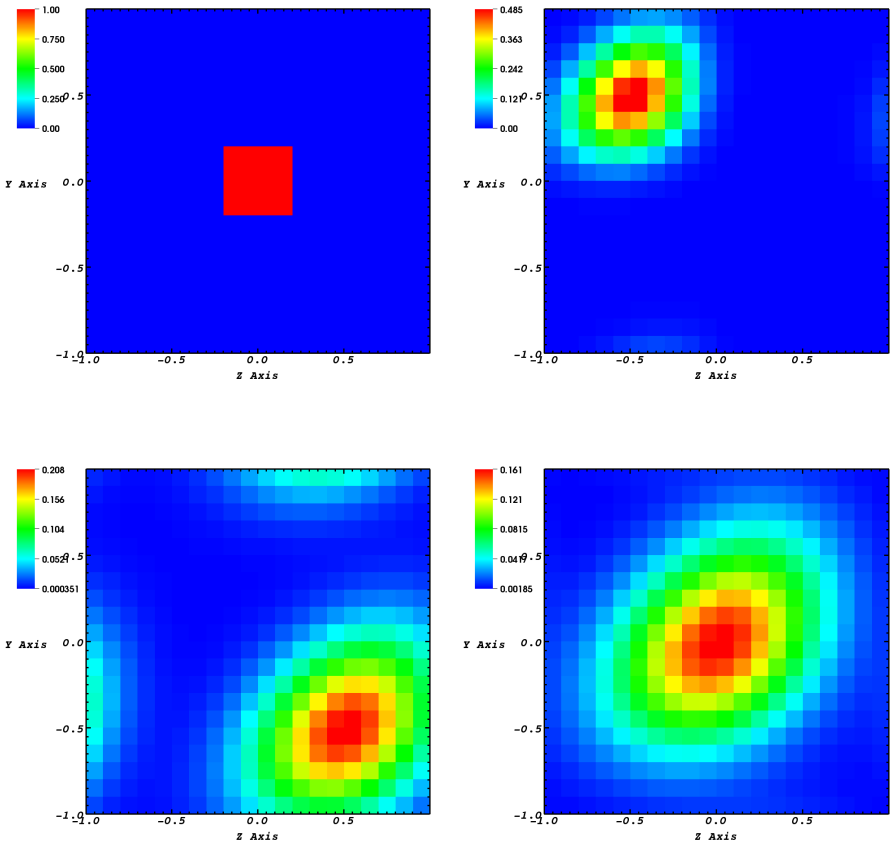

Figure 2: Propagation of B_x with a 1$^{\text{st}}$-order accurate field solver in a dense grid. The pictures show the initial state, and solutions after 10, 30, and 40 time steps with periodic boundary conditions. Maximum value at 80 time steps is 16.1% of initial value.

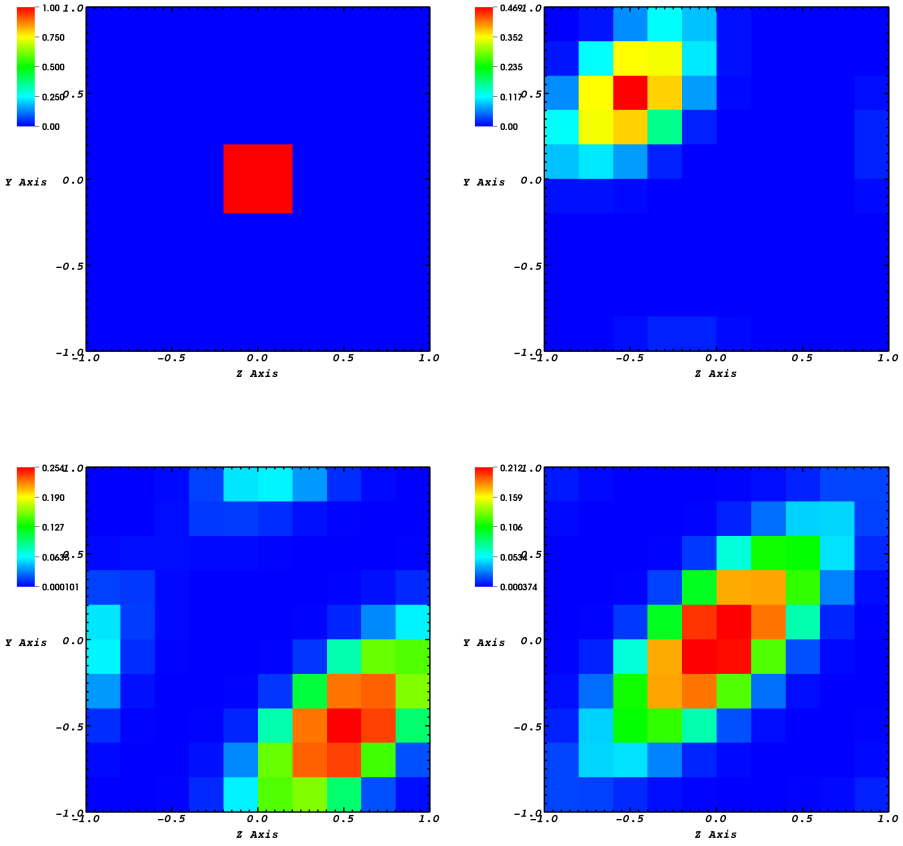

Figure 3: Propagation of B_x with a 2^{nd}-order accurate field solver in a sparse grid. The pictures show the initial state, and solutions after 10, 30, and 40 time steps with periodic boundary conditions. Maximum value at 40 time steps is 21.2% of initial value. Minmod limiter was used.

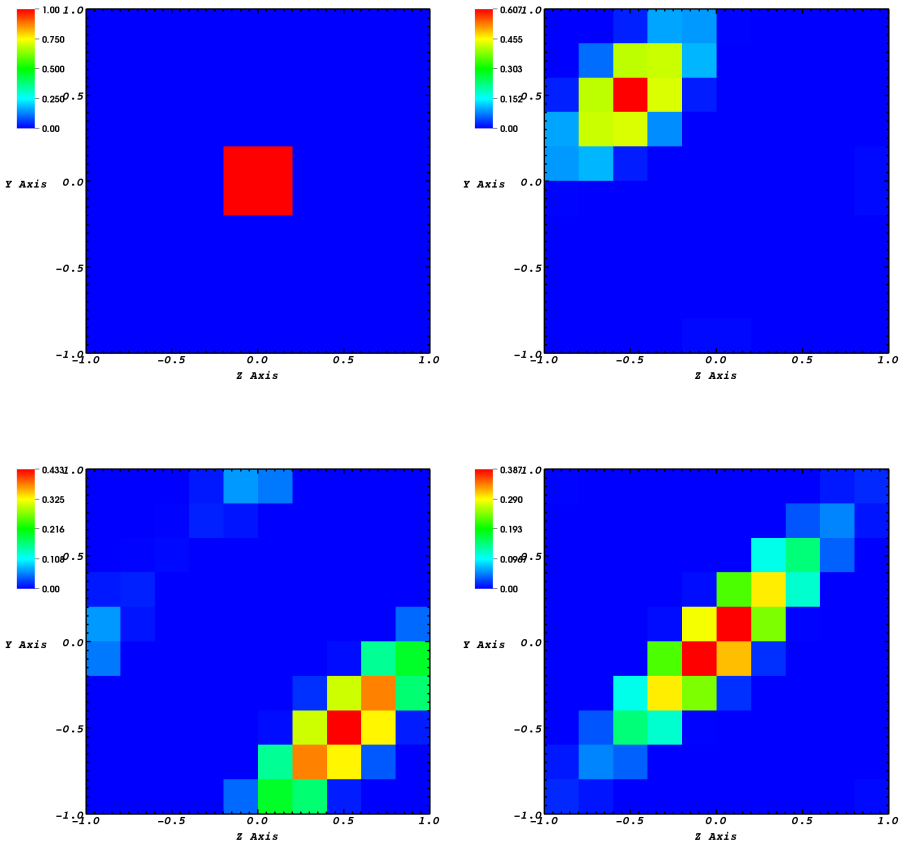

Figure 4: Propagation of B_x with a 2^{nd}-order accurate field solver in a sparse grid. The pictures show the initial state, and solutions after 10, 30, and 40 time steps with periodic boundary conditions. Maximum value at 40 time steps is 38.7% of initial value. MC limiter was used.

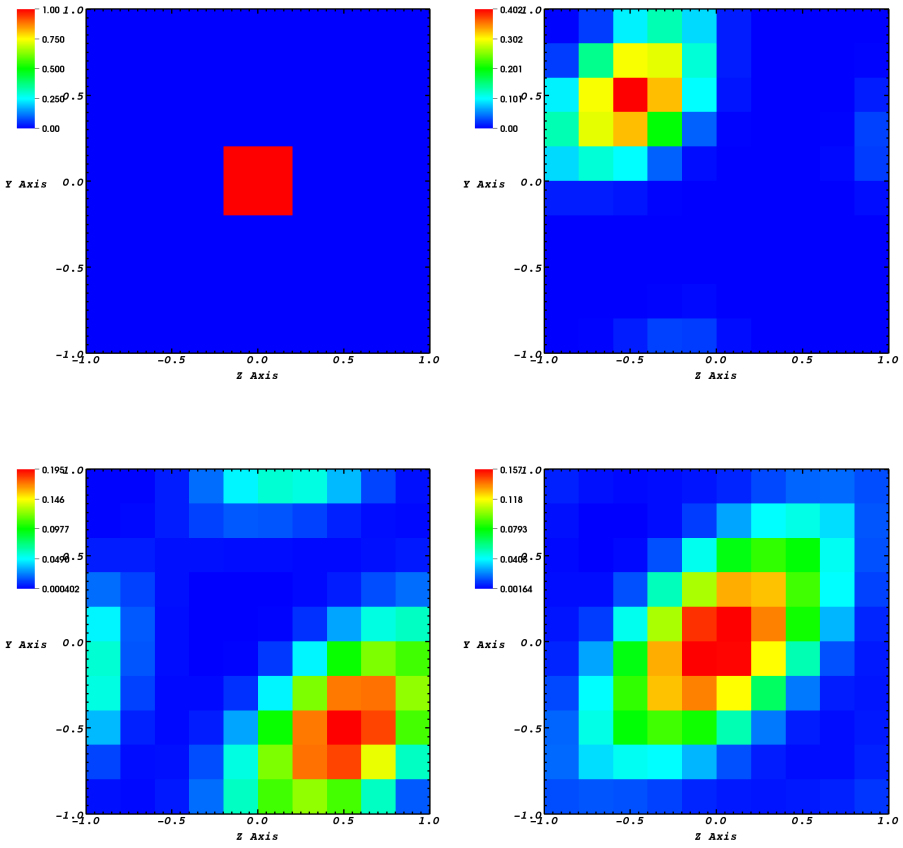

Figure 5: Propagation of B_x with a 2^{nd}-order accurate field solver in a sparse grid. The pictures show the initial state, and solutions after 10, 30, and 40 time steps with periodic boundary conditions. Maximum value at 40 time steps is 15.7% of initial value. Van Leer limiter was used.

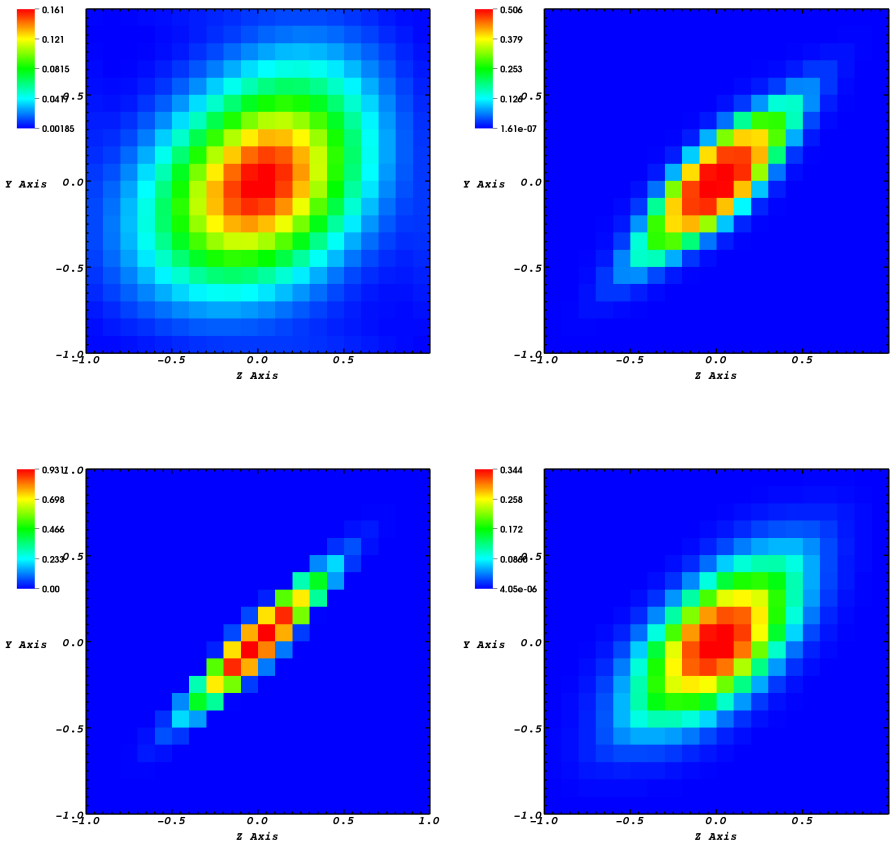

Figure 6: Numerical results of B_x propagation after 80 time steps in dense grid with (top left) 1$^{\text{st}}$-order accurate solver ($B_{x,\max} = 16.1\%$ of initial), and with 2$^{\text{nd}}$-order accurate solver with (top right) minmod limiter ($B_{x,\max} = 50.6\%$ of initial), (bottom left) MC limiter ($B_{x,\max} = 93.1\%$ of initial), (bottom right) Van Leer limiter ($B_{x,\max} = 34.4\%$ of initial).

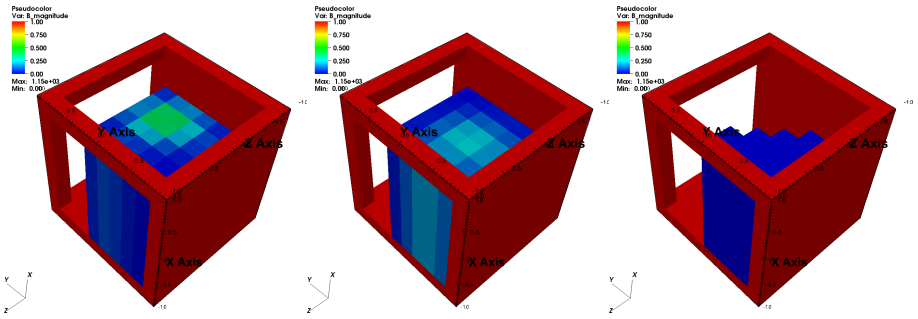

Figure 7: Propagation of B_x through the boundary of simulation domain with a constant velocity, using 1^{st}-order accurate solver. The panels show the numerical solution after 10 (left), 20 (middle), and 80 (right) time steps. Face-averaged B was set to value 666.0 on faces external to the simulation domain that should not affect the solution (cells drawn in red).

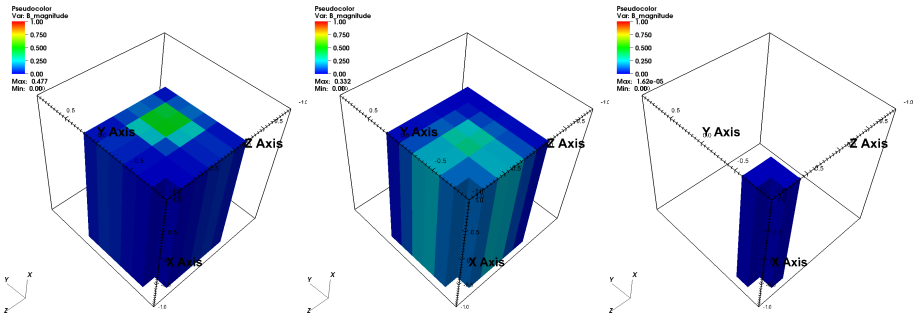

Figure 8: Propagation of B_x through the boundary of simulation domain with a constant velocity, using 2^{nd}-order accurate solver. The panels show the numerical solution after 10 (left), 20 (middle), and 80 (right) time steps. Here face-averaged B was set to zero value faces external to the simulation domain that should not affect the solution (cells drawn in red).